

## Supplementary Material

### **In-lipid structure of pressure sensitive domains hints mechanosensitive channel functional diversity**

C Kapsalis<sup>1</sup>, Y Ma<sup>2,4</sup>, BE Bode<sup>3\*</sup> and C Pliotas<sup>1,2,4\*</sup>

<sup>1</sup>*Biomedical Sciences Research Complex, School of Biology, University of St Andrews, UK*

<sup>2</sup>*Astbury Centre for Structural and Molecular Biology, University of Leeds, UK*

<sup>3</sup>*Biomedical Sciences Research Complex, School of Chemistry, University of St Andrews, UK*

<sup>4</sup>*School of Biomedical Sciences, Faculty of Biological Sciences, University of Leeds, UK*

\* corresponding author ([beb2@st-andrews.ac.uk](mailto:beb2@st-andrews.ac.uk) or [c.pliotas@leeds.ac.uk](mailto:c.pliotas@leeds.ac.uk))

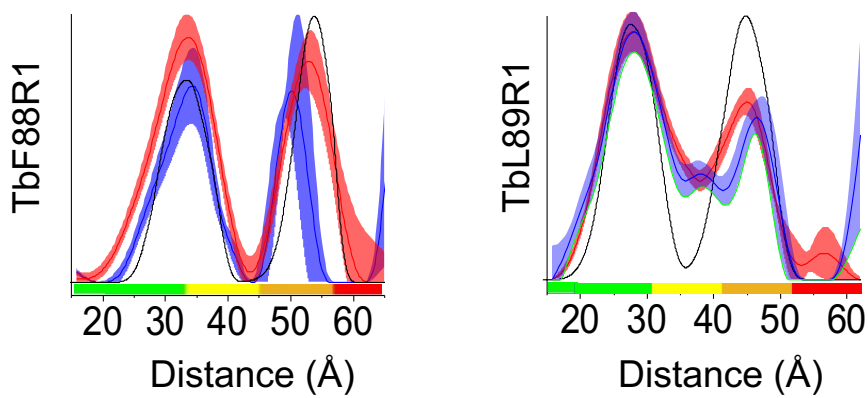


**Fig. S1:** Liposome (*E coli* polar extract) (shaded blue) and NDs (DMPC) (shaded red) PELDOR distance distributions compared to the modelled distances simulated from the x-ray (closed state) crystal structure (PDB 2OAR) using MtsslWizard (black line) for TbMscL F88R1 and L89R1.

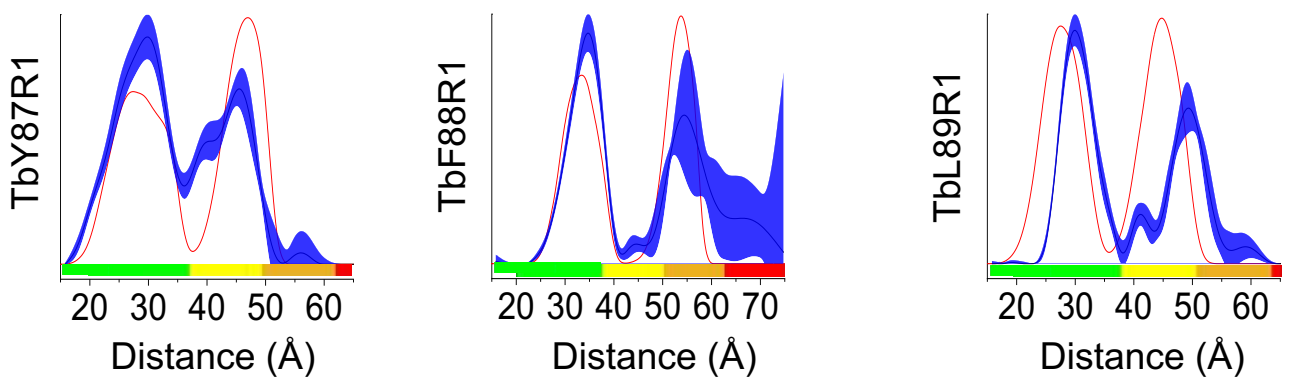


**Fig. S2:** PELDOR distance distributions of TbMscL in DDM (shaded blue) compared to the modelled distances simulated from the x-ray (closed state) crystal structure (PDB 2OAR) with MtsslWizard (red line).

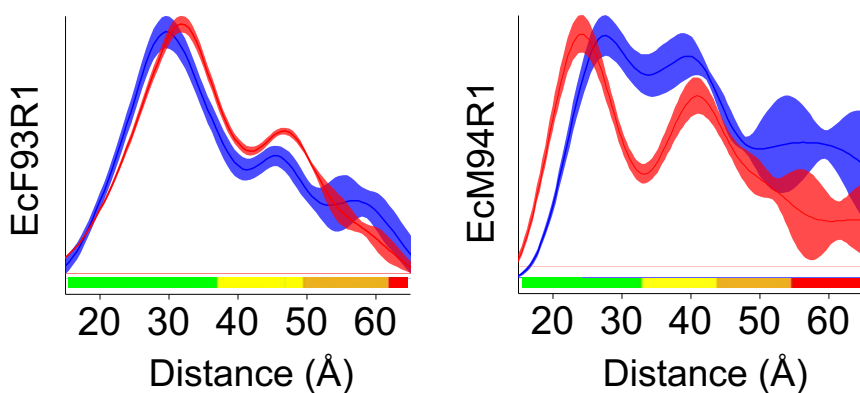


**Fig. S3:** EcMscL mutants PELDOR distance distribution comparison in DDM detergent (shade blue) and in nanodiscs (NDs) (shaded red).

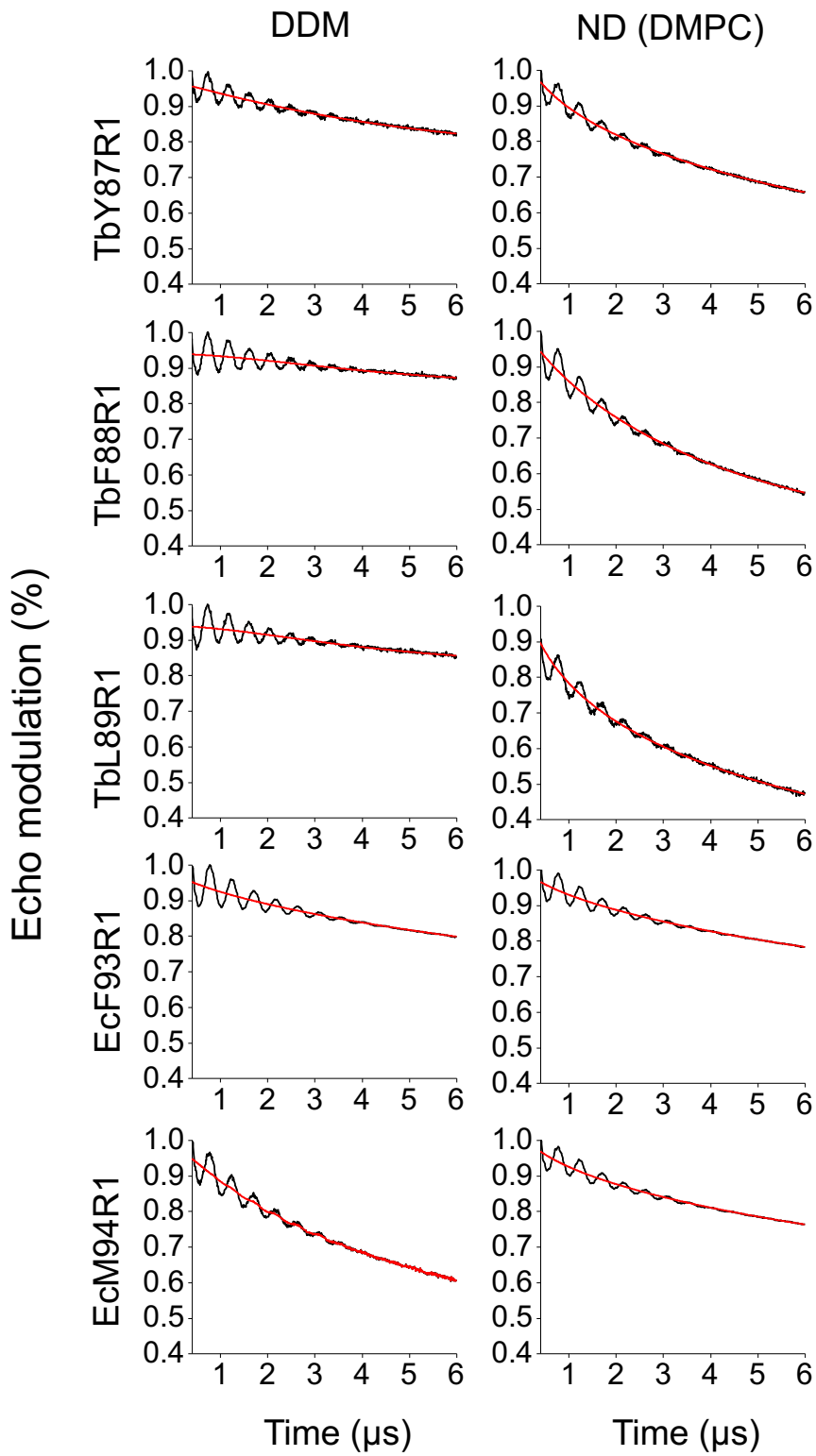


**Fig. S4:** Raw 3p-ESEEM data (black lines) and stretched exponential background fits (red lines).

		1	2	3	4	5
<i>M. tuberculosis</i>	1		29.45	21.66	29.75	68.99
<i>E. coli</i>	2	39		21.99	47.45	25.31
<i>M. acetivorans</i>	3	62	45		30.77	20.99
<i>S. aureus</i>	4	45	18	39		28.03
<i>M. leprae</i>	5	11	34	69	40	

**Table S1:** Pairwise alignment comparison between MscL orthologues. % sequence identity is shown in the upper/right half of the table and sequence residue gaps are shown in the lower/left half.

a.

Mutant	$D_1$ ; $D_2$ ; $D_2/D_1$ in DDM (Å)	$D_1$ ; $D_2$ ; $D_2/D_1$ in NDs (Å)
TbY87R1	29.7; 45.6; 1.55	26.3; 41.1; 1.57
TbF88R1	34.1; 55.8; 1.64	33.6; 53.1; 1.58
TbL89R1	30.0; 48.8; 1.63	27.8; 45.4; 1.63
EcF93R1	29.6; 45.8; 1.55	31.8; 46.9; 1.47
EcM94R1	27.7; 39.1; 1.41	24.1; 40.7; 1.69

b.

$D_1$ (TbL) – $D_1$ (EcL)	DDM (Å)	NDs (Å)
TbY87R1 - EcF93R1	0.1	-5.5
TbF88R1 - EcF93R1	4.5	1.8
TbF88R1 - EcM94R1	6.4	9.5
TbL89R1 - EcM94R1	2.3	3.7

**Table S2:** a.  $D_1$  and  $D_2$  PELDOR distance for each mutant in DDM and in nanodiscs (NDs) and their ratio. The expected ratios for symmetric multimers are 1.41 for a tetramer, 1.62 for a pentamer and 1.73 for a hexamer b.  $D_1$  distance differences between distinct mutants for the two orthologues.

<b>Mutant</b>	<b>% change in <sup>2</sup>H accessibility</b>
TbY87R1	(23±5)%
TbF88R1	(28±4)%
TbL89R1	(32±7)%
EcF93R1	-(27±4)%
EcM94R1	-(19±4)%

**Table S3:** Percentage (%) change in deuterium (solvent) accessibility of MscL in detergent (DDM) following reconstitution in Nanodiscs (DMPC).